CLASSIFICATION: **BIOLOGICAL SCIENCES (EVOLUTION)**

Title: A *Cerberus-Nodal-Lefty-Pitx* signalling cascade controls Left-Right asymmetry in amphioxus

Short title: Left-Right asymmetry in amphioxus

Guang Li[1, §], Xian Liu[1, §], Chaofan Xing[1], Huayang Zhang[1], Sebastian M. Shimeld[2*], Yiquan Wang[1*]

[1] State Key Laboratory of Cellular Stress Biology, School of Life Sciences, Xiamen University, Xiangan District, Xiamen, Fujian 361102, China
[2] Department of Zoology, University of Oxford, The Tinbergen Building, South Parks Road, Oxford OX1 3PS, UK
§ These authors contributed equally to this work.
* Corresponding authors: wangyq@xmu.edu.cn, sebastian.shimeld@zoo.ox.ac.uk

Key Words: Amphioxus; Nodal; Left-right asymmetry; TALEN

Significance statement

Some bilaterally symmetrical animals show genetically-programmed differences between their left and right sides, for example the placement of the heart and viscera in humans and other vertebrates. We dissect the regulation of this in embryos of amphioxus, a close relative of vertebrates which develops extraordinary asymmetries as a larva. We demonstrate a system in which asymmetric expression of the signal gene *Nodal* is controlled by positive and negative feedback loops with its own inhibitors. When this system is disrupted, embryos develop mirror-image symmetry with two 'left' sides or two 'right' sides. Comparison to other animals shows how this complex regulatory mechanism has evolved by addition of new feedback regulation to a more ancient signalling interaction.

Abstract

Many bilaterally symmetrical animals develop genetically-programmed left-right asymmetries. In vertebrates this process is under the control of Nodal signalling, which is restricted to the left side of the body by the Nodal antagonists Cerberus and Lefty. Amphioxus, the earliest diverging chordate lineage, has profound left-right asymmetry as a larva. We show that *Cerberus*, *Nodal*, *Lefty* and their target transcription factor *Pitx* are sequentially activated in amphioxus embryos. We then address their function by TALEN-based knockout and HSP promoter-driven overexpression. Knockout of *Cerberus* leads to ectopic right-sided expression of *Nodal*, *Lefty* and *Pitx*, while over expression of *Cerberus* represses their left-sided expression. Overexpression of *Nodal* in turn represses *Cerberus*, and activates *Lefty* and *Pitx* ectopically on the right side. We also show *Lefty* represses *Nodal*, while *Pitx* activates *Nodal*. These data combine in a model in which *Cerberus* determines whether the left-sided gene expression cassette is activated or repressed. We also show these regulatory steps are essential for normal left-right asymmetry to develop, as when they are disrupted embryos may instead form two phenotypic left sides or two phenotypic right sides. Our study shows the full regulatory cassette controlling left-right asymmetry was in place in the ancestor of amphioxus and vertebrates. This includes the deployment of the *Nodal* inhibitors *Cerberus* and *Lefty*, both of which operate in feedback loops with *Nodal* and combine to establish asymmetric *Pitx* expression. *Cerberus* and *Lefty* are missing from most invertebrate lineages, marking this mechanism as an innovation in the lineage leading to modern chordates.

/Body

Introduction

Bilaterians share three primary developmental axes. The Anterior-Posterior (AP) and Dorsal-Ventral (DV) axes define bilaterally-symmetrical organisation. The third axis, orthogonal to these, is known as the Medial-Lateral or Left-Right (LR) axis and displays mirror-image symmetry. However, many bilaterian species deviate consistently from true symmetry, raising fundamental questions of how symmetry is broken, and how different developmental programs can unfold on the left and right sides of an organism (1). In vertebrates this includes asymmetric development of the heart and viscera, disruption of which during embryogenesis causes a range of human disorders (2).

Correct LR organisation in vertebrates is regulated by a gene cassette in which right-sided *Cerberus* (*Cer*) and left-sided *Nodal* and *Lefty* regulate left-sided expression of the *Pitx* family gene *Pitx2*, and hence morphological LR asymmetry (3). *Cer* expression on the right of the embryonic node is required to repress Nodal signalling, which happens by Cer protein binding directly to Nodal protein. This restricts the ability of Nodal protein to activate the expression of the *Nodal* gene, leading to an upregulation of *Nodal* on the left of the embryo. *Lefty* expression is also upregulated by Nodal and, like Cer, acts as an extracellular inhibitor of Nodal. Co-expression of Nodal and Lefty can act as an activator-inhibitor system in the sense originally described by Turing (4). *Nodal* on the left of the embryo activates expression of *Pitx2*, which directs the development of left-sided morphology (3).

Several studies have sought to dissect the evolutionary history of *Nodal* signalling, and its regulation of LR asymmetry. Notably, asymmetric expression of *Nodal* and *Pitx* in gastropod mollusc embryos plays a role in the development of LR asymmetry, including the coiling of the shell (5, 6). Asymmetric expression of *Nodal* and/or *Pitx* has also been reported in some other lophotrochozoans, including *Pitx* in a brachiopod and an annelid, and *Nodal* in a brachiopod (7, 8). These data can be interpreted to suggest an ancestral role for *Nodal* and *Pitx* in regulating bilaterian LR asymmetry, however the picture is complicated by data from other lineages. First in ecdysozoan lineages *Nodal* appears to have been lost (7, 9), while *Pitx* is generally symmetrically expressed (8) and, where studied, does not function in LR asymmetry

(10, 11). Second, some lophotrochozoans do not show asymmetric Pitx expression (8, 12, 13). Third, functional studies on protostome Nodal signalling are currently restricted to molluscs (5), so it is unclear whether the regulatory connection between *Nodal* and *Pitx* is conserved even in those species that show asymmetric expression. An additional complication is that *Cer* and *Lefty* are also absent from many invertebrate bilaterian lineages (9, 14). The extracellular inhibition of Nodal by the proteins encoded by these two genes is a critical component of Nodal signalling in vertebrates (4, 15), and required both for the generation and maintenance of asymmetric *Nodal* and *Pitx2*.

To examine the evolutionary history of Nodal signalling and its regulation we turned to amphioxus, the basal chordate lineage and one that forms a typical chordate body plan while also developing pronounced LR asymmetries (16). During amphioxus embryogenesis the mouth opens on the left side of the head, while the gill slits, which initiate opening at the ventral midline, later extend up the right side. Other endodermal organs are similarly asymmetric, and somites also show pronounced LR asymmetry. *Cer, Nodal, Lefty* and *Pitx* are asymmetrically expressed in amphioxus, and pharmacological manipulation of the Alk4/5/7 Tgfβ receptor disrupts LR development, suggesting a function for Nodal in amphioxus LR asymmetry (17, 18). However *Nodal* function has not been directly tested, and it is not known if *Pitx* regulates LR asymmetric morphology. The functions of *Cer* and *Lefty* are also untested, so it is not clear if and how they regulate Nodal signalling.

To test these regulatory interactions in amphioxus we developed TALEN-based methods of removing gene function and Heat Shock Promoter (HSP) driven methods of overexpression, and deployed them to address the function of all four genes. We show that right-sided *Cer* represses *Nodal* expression, and find that when *Cer* function is impaired *Nodal* becomes bilateral. *Nodal* activates its own expression, and also that of *Lefty*. *Lefty* feeds back to repress *Nodal*, restricting its expression to the left side. This results in left-sided activation of *Pitx*. We further show that these regulatory steps are essential for normal left-right asymmetry to develop. The knockdown or overexpression of *Cer, Nodal, Lefty* of *Pitx* results in embryos with either two phenotypic left sides or two phenotypic right sides, with bilateral duplication of most normally lateralised structures in each case. These data show

the full regulatory cassette, with both inhibitors acting to restrict *Nodal* expression to the left side, is present in amphioxus and controls LR morphology. We conclude this pathway represents an ancient chordate character, with the full antagonist-based regulation of *Nodal* already present in the common ancestor of the chordates.

Results

Cer, *Nodal*, *Lefty* and *Pitx* are known to be asymmetrically expressed in amphioxus embryos (18-21), however the relative timing of their expression has yet to be elucidated. We therefore examined whether these genes are spatiotemporally activated in patterns consistent with a regulatory hierarchy. Staged *in situ* hybridisation demonstrated that right-sided *Cer* preceded lateral restriction of *Nodal, Lefty*, and *Pitx* (*SI Appendix*, Fig. S1). Furthermore, lateralised expression of *Lefty* and *Pitx* preceded that of *Nodal* (*SI Appendix*, Fig. S1).

These temporal expression patterns are consistent with Cer regulating the lateralisation of the other genes. To test this we generated a TALEN knockout heterozygous *Cer* line (*SI Appendix*, Fig. S2, S3). Crossing $Cer^{+/-}$ animals yielded $Cer^{+/+}$, $Cer^{+/-}$ and $Cer^{-/-}$ genotypes in the expected ratio (*SI Appendix*, Fig. S4), and we assessed the expression of *Nodal*, *Lefty* and *Pitx* in these embryos. While $Cer^{+/-}$ and wild type embryos maintained wild type expression, $Cer^{-/-}$ embryos showed bilateral expression of *Nodal*, *Lefty* and *Pitx* (Fig. 1a-f). This indicates Cer is necessary to restrict the expression of Nodal, Lefty and Pitx to the left side of amphioxus embryos. To test whether Cer was also sufficient to regulate these genes, we induced overexpression of *Cer* using a heat-regulated *HSP::Cer* construct (*SI Appendix*, Fig. S5). This generated widespread ectopic *Cer* expression in 100% (31/31) of embryos (Fig. 1h), and abolished left-sided expression of *Nodal*, *Lefty* and *Pitx* in 100% (84/84), 95% (80/88) and 66% (46/70) of embryos respectively (Fig. 1j, l, n). Combined, these data show *Cer* is necessary and sufficient for regulating the lateral expression of *Nodal*, *Lefty* and *Pitx*.

Nodal signalling is transduced by Tgfβ receptors of the Alk4/5/7 family (22). Pharmacological inhibition of Alk4/5/7 in amphioxus has been reported to block left-sided *Nodal*, *Lefty* and *Pitx* expression (18), and we found the same in our experiments (Fig. 2b, f, h). However the Alk4/5/7 receptor may also mediate

signalling by other Tgfβ family ligands, including Activin and Tgfβ (23), raising uncertainty as to the ligand involved in its activation in amphioxus *in vivo*. *Nodal* in amphioxus also has an earlier developmental role (24), precluding its inhibition by the TALEN method as embryos would not develop to the stage where LR asymmetry can be addressed. We therefore tested the effect of inducible and ectopic Nodal on amphioxus LR asymmetry. Overexpression of *Nodal* using an *HSP::Nodal* construct (Fig. 2r, t, v; *SI Appendix*, Fig. S5), or administration of Nodal protein to developing embryos (Fig. 2j, n, p), induced ectopic right-sided expression of *Nodal*, *Lefty* and *Pitx*. We also found that *Nodal* manipulation fed back on *Cer* expression, with Alk4/5/7 inhibition inducing ectopic left-sided *Cer* (as previously reported (18)), and Nodal overexpression inhibiting *Cer* expression in the first somites (Fig. 2d, l). These results confirm previous inference of the necessity of Nodal for lateralised Pitx expression in amphioxus, demonstrate that it is also sufficient, and further show that Nodal also negatively regulates *Cer* expression. Since we have shown that *Cer* inhibits *Nodal*, this suggests a negative feedback loop in which *Nodal* represses the expression of its own inhibitor.

In vertebrate embryos, Lefty also acts as an extracellular inhibitor of Nodal protein, and experiments in an echinoderm suggest this might also be the case in this lineage (25). To test the function of *Lefty* in amphioxus, we generated embryos in which the *Lefty* gene was targeted by injection of a TALEN mRNA (*SI Appendix*, Fig. S6). In 82.4% (98/118) of injected embryos *Nodal* expression became bilateral (Fig. 3d). Furthermore *Pitx* and *Lefty* itself also became bilateral, in 49.3% (102/207) and 36.7% (40/109) of embryos respectively (Fig. 3h, f). To test the sufficiency of *Lefty* to inhibit normal left-sided gene expression we also injected embryos with an inducible *HSP::lefty* construct (*SI Appendix*, Fig. S5). In the majority of heat shocked embryos left-sided expression of *Nodal* and *Pitx* was lost (Fig. 3l, n). These data demonstrate that, in amphioxus, *Lefty* can act to inhibit *Nodal*. In the absence of *Lefty*, *Nodal* is ectopically expressed on the right hand side (Fig. 3d). As *Nodal* upregulates *Lefty* and *Pitx* (Fig. 2n, p, t, v), this probably in turn leads to the ectopic expression of *Lefty* and *Pitx* seen in *Lefty* TALEN injected embryos (Fig. 3f, h).

Pitx homeobox genes are conserved targets of Nodal signalling in vertebrates (3), echinoderms (26) and probably also molluscs (5). In vertebrates asymmetric *Pitx2* is

required for correct LR morphogenesis, but studies suggest that *Pitx2* does not feed back to regulate *Nodal* expression (27). While the experiments described above show that *Cer*, *Lefty* and *Nodal* can regulate *Pitx* in amphioxus, they do not establish whether *Pitx* might also regulate their expression. To test this we sought to up- and downregulate *Pitx* expression, while monitoring its impact on the expression of *Nodal* and *Lefty*. Upregulation of *Pitx* by mRNA injection caused significant disruption to early development, though many of the embryos that did survive through to the neurula stage and beyond displayed ectopic right-sided expression of *Nodal* (45.3%: 24/53) and *Lefty* (20.5%: 9/44) (Fig. 3b', d'). To abrogate this early developmental impact of *Pitx* mRNA injection, we injected an inducible *HSP::Pitx* construct (*SI Appendix*, Fig. S5). In heat-induced *HSP::Pitx* injected embryos, 16.5% (19/115) showed ectopic right sided *Nodal* expression (Fig. 3h'). None showed ectopic *Lefty* expression (Fig. 3j'). To block *Pitx* function, we designed a fusion construct linking amphioxus Pitx DNA-binding domain to the Engrailed Repressor (EnR) domain (*SI Appendix*, Fig. S5), and injected the mRNA encoding this into amphioxus embryos. As with *Pitx* mRNA injection, many such embryos developed with significant abnormalities prior to the neurula stage, precluding their analysis for LR defects. However, in embryos that reached the neurula stage and displayed approximately normal AP and DV axial organisation, ectopic activation of both *Lefty* and *Nodal* was observed on the right side in 71.4% (5/7) and 42.9% (6/14) of cases respectively (Fig. 3n', l').

In some cases, LR asymmetry phenotypes derived from manipulating gene expression early in development might be explained by disturbed AP/DV organisation, which in vertebrates may affect the midline and hence increase the incidence of laterality defects (28). While this consideration might apply to embryos injected with *Pitx* mRNA or *Pitx-EnR* mRNA, which would be translated very early in development, the *HSP::Pitx* construct was only activated by heat shock after the mid-gastrula stage, and this also induced ectopic right-sided *Nodal* expression (Fig. 3h'). These data suggest that, unlike vertebrates, in amphioxus *Pitx* feeds back to regulate Nodal signalling.

The experiments described above show that *Cer* represses *Nodal*, that Nodal represses *Cer* and activates *Lefty* and *Pitx*, that *Lefty* represses *Nodal*, and that *Pitx*

activates *Nodal*. An assumption is that left-sided *Pitx* will drive the development of left-sided morphology. To test this we allowed embryos in which *Cer, Nodal, Lefty* or *Pitx* expression had been manipulated to grow to the late embryonic or larval stages, so we could monitor the impact on the development of LR asymmetric characters.

Amphioxus larvae are extremely asymmetric, with the mouth positioned on the left side of the head, and the gill slits, which initiate opening at the ventral midline, expanding to spread up the right side. Several internal systems are also distinctly organised across the LR axis of the head and pharynx, including the club-shaped gland, pre-oral pit and endostyle (Fig. 4a-c). A suit of asymmetrically expressed marker genes (18) including *Krox*, *FoxE4*, *Nkx2*.1, *Pit* and *Dkk1/2/4* mark the LR displacement of these structures (Fig. 4a', e', I', m', q'). To determine the impact of manipulating *Cer* expression on LR morphology, we allowed manipulated embryos to grow to the larval stage before analysing morphology and LR marker gene expression. *Cer*$^{-/-}$ embryos develop a consistent two left sides (2-left) phenotype, with a mouth opening on each side, duplication of the left-sided structures such as the pre-oral pit and proximal club shaped gland, and loss of the right-sided distal club-shaped gland (Fig. 4d-f; *SI Appendix*, Fig. S7). The gill slits, while still initiating and opening at the ventral midline, were also affected as they failed to extend up the right side (Fig. 4d-f; *SI Appendix*, Fig. S7). Conversely, *HSP::Cer* larvae developed the reciprocal phenotype, with two right sides (2-right) and concomitant duplication of most right-sided structures (Fig. 4g-l; *SI Appendix*, Fig. S7). The gill slits were also affected: The first slit appeared to initiate at the ventral midline and like the *Cer*$^{-/-}$ phenotype failed to extend up either side, however unlike *Cer*$^{-/-}$ embryos it also failed to properly open. LR marker gene expression precisely matched this morphology, confirming the duplication and loss of reciprocal structures in the 2-left and 2-right phenotypes (Fig. 4a'-t'). We also allowed embryos in which *Nodal* or *Lefty* had been up- or downregulated to grow to the larval stage. These manipulations also produced embryos with asymmetry defects, with *Nodal* overexpression and *Lefty* knockdown resulting in 2-left phenotypes, and *Nodal* knockdown or *Lefty* overexpression resulting in 2-right phenotypes (*SI Appendix*, Fig. S7). As discussed above, injection of *Pitx* mRNA caused early developmental malformations, however a small number of such embryos did pass through to the larval stage and among them 6.1% exhibited 2-left phenotypes. Likewise, *Pitx* overexpression via the *HSP::Pitx*

construct, which did not affect early development, also produced 2-left phenotypes in 10.2% of cases. No 2-right phenotypes were observed in either manipulation. Embryos injected with *Pitx-EnR* were severely malformed by the larval stage and few pharyngeal structures could be discerned. However in 7% of cases paired bilateral mouths were observed, approximating the 2-left phenotype. This is consistent with the ectopic right sided activation of *Nodal* in *Pitx-EnR* injected embryos (Fig. 3l', n'). These data indicate that the asymmetric expression of the *Cer-Nodal-Lefty-Pitx* cassette regulates the LR morphology of the larva in a predictable way: any side on which *Nodal-Pitx* are activated becomes phenotypically left. If they are not activated, it becomes phenotypically right.

Discussion

This study shows that the *Cer-Nodal-Lefty-Pitx* cassette functions in amphioxus to regulate LR asymmetry. Our data allow us to construct a regulatory model for the left and right side of amphioxus embryos (Fig. 5). The model suggests competitive feedback on the left side of the amphioxus embryo, with Nodal repressing the expression of its upstream repressor (*Cer*), while activating the expression of its downstream repressor (*Lefty*) and activator (*Pitx*). In vertebrates both Cer and Lefty repress *Nodal* signalling by directly binding to Nodal protein, while Nodal upregulates its own expression and that of *Lefty* (4, 15). Thus, in both lineages, the establishment of LR identify is dependent on the appropriate regulation of Nodal via positive and negative feedback mediated by extracellular factors. Their focus is establishing asymmetric *Pitx* as the downstream effector, and disruption of this process in amphioxus or vertebrates leads to embryos with disrupted LR asymmetry. The morphological outcome in amphioxus is predictable based upon the gene expression; essentially if *Pitx* expression is activated on a side of the embryo, it will develop left sided morphology, while if *Pitx* is absent, right-sided morphology will develop. Manipulations which yield bilateral *Pitx* distributions generate unviable embryos with 2-left or 2-right sided organisation, with duplication of the respective pharyngeal and endodermal structures including the mouth, endostyle and club-shaped gland. These morphologies show that, once handedness is established in amphioxus, the two sides develop independently and autonomously according to their gene expression, and are not noticeably influenced by what is happening on the other side of the embryo.

While the core *Cer-Nodal-Lefty-Pitx* pathway appears conserved between amphioxus and vertebrates, we also note a difference: in amphioxus *Pitx* feeds back on the regulation of *Nodal* expression. Our model (Fig. 5) suggests that in amphioxus the propagation of 'leftness' downstream of asymmetric *Nodal* may therefore depend on competition between positive feedback from *Pitx* and negative feedback from *Lefty*. This regulatory link is not seen in vertebrates or echinoderms (where *Nodal* regulation of *Pitx* has been demonstrated (26)), suggesting it may be an amphioxus novelty.

There are also some aspects of amphioxus morphology that our work sheds light on. The amphioxus mouth is unusual in that it opens on the left side of the head, rather than the midline as in most animal lineages, including vertebrates. This has led to speculation that the amphioxus mouth is a derived structure, possibly evolving from the equivalent of a left-sided coelomic pore, and not homologous to mouths in other chordates (17). Our demonstration of its dependence on the *Cer-Nodal-Lefty-Pitx* pathway supports this theory, as the mouth is regulated as a left-sided rather than a midline structure.

Amphioxus gill slits are also unusual. The first gill slit openings, known as the primary gill slits, appear first at the ventral midline then extend only up the right side of the head (29). Through larval development gill slits are hence right-sided only. However at metamorphosis another set of gill slit openings appear, known as the secondary gill slits. These initiate also on the right side of the larva, dorsal to the primary slits. As these secondary slits extend, the primary slits move ventrally and eventually come to lie on the left side of the head, such that the final adult morphology has symmetrical gill slits. This has led to an assumption, dating from the 1800's, that the slits that lie on the right side of the larval head are in fact homologous to the left-sided slits in other deuterostomes (30). In our experiments the primary slits initiate, but fail to extend in 2-left embryos, or to open at all in 2-right embryos. That they initiate is consistent with their positioning at the ventral midline, suggesting this does not require LR axial information. Failure to extend in either sort of embryo suggests subsequent morphogenesis requires both left- and right-sided information. Furthermore, that the slits develop further in 2-left embryos than in 2-

right embryos is in keeping with the historical view that the primary slits are, primitively, left-sided structures.

We do not know what breaks symmetry in amphioxus. Studies in some vertebrates, in the urochordate *Halocynthia*, and in echinoderms, suggest a role for cilia in symmetry breaking (31-33). While the amphioxus embryo is heavily ciliated at the stages at which the model suggests symmetry is broken, as yet there is no evidence for a functional role for cilia in amphioxus, though we consider the timing of expression and regulatory interactions consistent with the proposal by Blum and colleagues for a cilia-based mechanism localised to the gastrocoel roof (31). Whatever the symmetry-breaking mechanism, our data suggest it might work in two ways. Symmetric *Cer* precedes asymmetric right-sided *Cer*. This in turn precedes asymmetric *Nodal* expression, but asymmetric *Lefty* and *Pitx* expression are detectable before asymmetric *Nodal* expression, yet are regulated by *Nodal*. Thus the symmetry breaking mechanism might act to repress *Cer* expression on the left, allowing Nodal protein to activate *Lefty* and *Pitx*. *Nodal* autoregulates, explaining the lag in asymmetric *Nodal* expression comparted to *Lefty* and *Pitx*. Under this model *Nodal* negative feedback on *Cer* would act to lock in this state. We do not know precisely how *Nodal* feeds back on *Cer*, though inhibition of the Alk4/5/7 receptor shows it works through this pathway.

The second possibility is that, as *Nodal* feeds back negatively on *Cer*, the symmetry breaking mechanism might act to liberate *Nodal* from *Cer* repression. Since Cer represses Nodal by direct protein-protein binding (15), this could be via some additional extracellular factor preventing or disrupting this interaction. Under this model Nodal would then repress *Cer*, and regulate *Lefty* and *Pitx* as above. While compatible with much of our data, this does not easily account for the early onset of asymmetric *Cer* compared to *Lefty* and *Pitx*. It is also not how the system is thought to work in vertebrates (Fig. 5), where there is so far no evidence for *Nodal* feeding back on *Cer*. We hence consider it a less parsimonious explanation.

Our study shows that full complexity of the *Cer-Nodal-Lefty-Pitx* cassette was established by the common ancestor of the chordates and inherited by their vertebrate descendants. *Pitx* and *Nodal* are also involved in LR specification in

molluscs (5) and may be asymmetrically expressed in some other lophotrochozoans (7, 8), leading to speculation that the role of *Nodal* signalling in LR development was acquired early in animal evolution. However the roles of *Cer* and *Lefty* may be more recent innovations. *Cer* is a member of the larger Cer/DAN/Gremlin family of Tgfβ signalling regulators. Clear *Cer* genes have only been identified in chordates, though one study suggests they may be older and lost by many lineages (9). *Lefty* is a divergent member of the Tgfβ family. It is so far found only in chordates and ambulacrarians, and in the latter does function in LR asymmetry (9, 25). Therefore it is unlikely that *Cer* and *Lefty* are more broadly involved in LR asymmetry across protostomes, and we suggest their incorporation into regulation of LR asymmetry are innovations of chordates and deuterostomes respectively, with negative feedback providing more nuanced control of Nodal signalling in these lineages.

Materials and Methods

Animal and embryo cultivation and embryo microinjection

Amphioxus (*Branchiostoma floridae*) were originally acquired from Jr-Kai Yu, and the colony was maintained under previously-described conditions (34, 35). Gametes were obtained using the thermal-shock method (from 20˚C to 26 ˚C)(34). Fertilization and subsequent culturing of the embryos were carried out essentially as described previously (36) at 27-28 ˚C unless otherwise stated. Injection solution was prepared containing 20% glycerol, 5 mgmL^{-1} Texas Red dextran (Life Technology Co.), and 0.25 μgμL^{-1} plasmid DNA or 0.15-1.5μgμL^{-1} synthesized mRNA. Embryo microinjection was performed as previously described (36).

Larval cultivation and detection of *Cer* mutations in founder and F1 amphioxus.

Cer Talen mRNA-injected embryos and larvae were reared at 24˚C and fed with unicellular algae *Dicrateria zhanjiangensis*, and juveniles and adults were reared in a same way as previous description (34, 35). Each F0 founder was crossed with a wild-type animal respectively. About 30-50 embryos of each cross were collected and lysed with Animal Tissue Direct PCR Kit (Foregene Co., China) for mutation efficiency and mutation site analysis (34). Progeny of crosses carrying frame-shift mutations were maintained. F1 genotypes were determined in a similar way as

described for F0 by cutting a tiny tip of the tail of each animal. The F1 animals carrying identical frame-shift mutations were maintained and inter-crossed to generate F2 generation. The F2 embryos were fixed at different developmental stages with 4% PFA-MOPS-EGTA for in situ hybridization analysis or morphological examination. Animal husbandry and mutation detection are described in detail in *SI Appendix, Materials and Methods*.

Plasmid construct preparation

The full-length of coding sequences of *Cer*, *Nodal*, *Lefty* and *Pitx* genes were amplified from a gastrula cDNA library and then ligated into a pGEM-T-Easy vector (Promega Co.) separately. Further, they were recombined into exression vectors pXT7 or P1. The P1 is a construct initially derived from vector pAcGFP1-1 (Clontech Co.) by integrating a 790 bp regulatory region of *B*. *belcheri Hsp70* gene upstream the GFP coding sequence (37). A *Pitx-EN* dominant negative construct was made by fusing the Pitx DNA-binding domain and the *Drosophila* Engrailed repressor domain (EnR) in the pXT7 vector. Talens targeting *Cer* and *Lefty* genes were designed and assembled as previously described (38). TALEN binding sites and primer sequences used for cloning and Talen efficiency assay are shown in *SI Appendix*, Tables S1-S5. The details for the preparation are described in *SI Appendix, Materials and Methods*.

In vitro synthesised mRNA and plasmid DNA preparation

All plasmid DNAs were prepared using Plasmid Mini Kit (Omega Co.) and linearized with either *BamH*I (for pXT7-derived constructs) or SacI (for Talen constructs), extracted by phenol-chloroform and dissolved in RNase-free water. *In vitro* mRNA synthesis was conducted using either T7 (for pXT7-derived constructs) or T3 (for Talen constructs) using mMESSAGE mMACHINE kit (Ambion Co.).

Heat-shock experiment

Embryos injected with *Hsp70::Cer*, *Hsp70::Nodal*, *Hsp70::Lefty* or *Hsp70::Pitx* DNA plasmids were raised at 25 ˚C, until they developed to early gastrula stage, when half were heat-shocked at 34 ˚C in a water bath for 30 minutes and the rest were left at 25 ˚C as controls. After heat shock, the embryos were returned to 25 ˚C and

allowed to develop until they were fixed with 4% PFA-MOPS-EGTA at desired stages for *in situ* or morphological analysis.

SB505124 and Nodal protein treatment

Embryos were treated with 50 μM SB505124 (Sigma Co.) or 1-8 μgml^{-1} recombinant mouse Nodal protein (R&D Co.) in four-well dishes (coated with 1.5% agarose) from early gastrula to 8-somite stages, or from 3-/5-somite to 8-somite stages, and then were fixed at required stages for *in situ* hybridization or cultured continuously for morphological observation. The experiments of *in situ* hybridization (WISH) were performed essentially according to the previous description (39). All details are described in *SI Appendix, Materials and Methods*.

Acknowledgements

We thank Dr. Jr-Kai Yu at the Institute of Cellular and Organismic Biology, Academia Sinica for providing *B. floridae* animals and Dr Dominic Norris for comments on the manuscript. This work was supported by grants from National Natural Science Foundation of China (No. 31471986, No. 31372188 and No. 31672246) and from the Fundamental Research Funds for the Central Universities of China (No. 20720150201).

References

1. Palmer AR (2004) Symmetry breaking and the evolution of development. *Science* 306(5697):828-833.
2. Bisgrove BW, Morelli SH, & Yost HJ (2003) Genetics of human laterality disorders: insights from vertebrate model systems. *Annu Rev Genomics Hum Genet* 4:1-32.
3. Vandenberg LN & Levin M (2013) A unified model for left-right asymmetry? Comparison and synthesis of molecular models of embryonic laterality. *Dev Biol* 379(1):1-15.
4. Muller P*, et al.* (2012) Differential diffusivity of Nodal and Lefty underlies a reaction-diffusion patterning system. *Science* 336(6082):721-724.
5. Grande C & Patel NH (2009) Nodal signalling is involved in left-right asymmetry in snails. *Nature* 457(7232):1007-1011.
6. Kuroda R, Endo B, Abe M, & Shimizu M (2009) Chiral blastomere arrangement dictates zygotic left-right asymmetry pathway in snails. *Nature* 462(7274):790-794.
7. Grande C, Martin-Duran JM, Kenny NJ, Truchado-Garcia M, & Hejnol A (2014) Evolution, divergence and loss of the Nodal signalling pathway: new data and a synthesis across the Bilateria. *Int J Dev Biol* 58(6-8):521-532.
8. Martin-Duran JM, Vellutini BC, & Hejnol A (2016) Embryonic chirality and the evolution of spiralian left-right asymmetries. *Philos Trans R Soc Lond B Biol Sci* 371(1710).
9. Kenny NJ*, et al.* (2014) The Lophotrochozoan TGF-beta signalling cassette - diversification and conservation in a key signalling pathway. *Int J Dev Biol* 58(6-8):533-549.

10. Vorbruggen G*, et al.* (1997) Embryonic expression and characterization of a Ptx1 homolog in Drosophila. *Mech Dev* 68(1-2):139-147.
11. Westmoreland JJ, McEwen J, Moore BA, Jin Y, & Condie BG (2001) Conserved function of Caenorhabditis elegans UNC-30 and mouse Pitx2 in controlling GABAergic neuron differentiation. *J Neurosci* 21(17):6810-6819.
12. Currie KW & Pearson BJ (2013) Transcription factors lhx1/5-1 and pitx are required for the maintenance and regeneration of serotonergic neurons in planarians. *Development* 140(17):3577-3588.
13. Marz M, Seebeck F, & Bartscherer K (2013) A Pitx transcription factor controls the establishment and maintenance of the serotonergic lineage in planarians. *Development* 140(22):4499-4509.
14. Namigai EK, Kenny NJ, & Shimeld SM (2014) Right across the tree of life: the evolution of left-right asymmetry in the Bilateria. *Genesis* 52(6):458-470.
15. Piccolo S*, et al.* (1999) The head inducer Cerberus is a multifunctional antagonist of Nodal, BMP and Wnt signals. *Nature* 397(6721):707-710.
16. Boorman CJ & Shimeld SM (2002) The evolution of left-right asymmetry in chordates. *Bioessays* 24(11):1004-1011.
17. Kaji T, Reimer JD, Morov AR, Kuratani S, & Yasui K (2016) Amphioxus mouth after dorso-ventral inversion. *Zoological Lett* 2:2.
18. Soukup V*, et al.* (2015) The Nodal signaling pathway controls left-right asymmetric development in amphioxus. *Evodevo* 6:5.
19. Onai T, Yu JK, Blitz IL, Cho KW, & Holland LZ (2010) Opposing Nodal/Vg1 and BMP signals mediate axial patterning in embryos of the basal chordate amphioxus. *Dev Biol* 344(1):377-389.
20. Yasui K, Zhang S, Uemura M, & Saiga H (2000) Left-right asymmetric expression of BbPtx, a Ptx-related gene, in a lancelet species and the developmental left-sidedness in deuterostomes. *Development* 127(1):187-195.
21. Yu JK, Holland LZ, & Holland ND (2002) An amphioxus nodal gene (AmphiNodal) with early symmetrical expression in the organizer and mesoderm and later asymmetrical expression associated with left-right axis formation. *Evol Dev* 4(6):418-425.
22. Reissmann E*, et al.* (2001) The orphan receptor ALK7 and the Activin receptor ALK4 mediate signaling by Nodal proteins during vertebrate development. *Genes Dev* 15(15):2010-2022.
23. Moustakas A & Heldin CH (2009) The regulation of TGFbeta signal transduction. *Development* 136(22):3699-3714.
24. Yu JK*, et al.* (2007) Axial patterning in cephalochordates and the evolution of the organizer. *Nature* 445(7128):613-617.
25. Duboc V, Lapraz F, Besnardeau L, & Lepage T (2008) Lefty acts as an essential modulator of Nodal activity during sea urchin oral-aboral axis formation. *Dev Biol* 320(1):49-59.
26. Duboc V, Rottinger E, Lapraz F, Besnardeau L, & Lepage T (2005) Left-right asymmetry in the sea urchin embryo is regulated by nodal signaling on the right side. *Dev Cell* 9(1):147-158.
27. Ryan AK*, et al.* (1998) Pitx2 determines left-right asymmetry of internal organs in vertebrates. *Nature* 394(6693):545-551.
28. Roessler E & Muenke M (2001) Midline and laterality defects: left and right meet in the middle. *Bioessays* 23(10):888-900.
29. Hatschek B (1881) Entwicklung des Amphioxus. *Arbeiten aus dem Zoologischen Institut Wien* IV(Heft 1):1-88 + plates.
30. Willey A (1894) *Amphioxus and the ancestry of the vertebrates* (Macmillan and Co., New York).
31. Blum M, Feistel K, Thumberger T, & Schweickert A (2014) The evolution and conservation of left-right patterning mechanisms. *Development* 141(8):1603-1613.

32. Nishide K, Mugitani M, Kumano G, & Nishida H (2012) Neurula rotation determines left-right asymmetry in ascidian tadpole larvae. *Development* 139(8):1467-1475.
33. Tisler M*, et al.* (2016) Cilia are required for asymmetric nodal induction in the sea urchin embryo. *BMC Dev Biol* 16(1):28.
34. Li G, Shu Z, & Wang Y (2013) Year-round reproduction and induced spawning of Chinese amphioxus, Branchiostoma belcheri, in laboratory. *PLoS One* 8(9):e75461.
35. Li G, Yang X, Shu Z, Chen X, & Wang YQ (2012) Consecutive spawnings of Chinese amphioxus, Branchiostoma belcheri, in captivity. *PLoS One* 7(12):e50838.
36. Liu X, Li G, Feng J, Yang X, & Wang YQ (2013) An efficient microinjection method for unfertilized eggs of Asian amphioxus Branchiostoma belcheri. *Dev Genes Evol* 223(4):269-278.
37. Li D*, et al.* (2012) Isolation and functional analysis of the promoter of the amphioxus Hsp70a gene. *Gene* 510(1):39-46.
38. Li G*, et al.* (2014) Mutagenesis at specific genomic loci of amphioxus Branchiostoma belcheri using TALEN method. *J Genet Genomics* 41(4):215-219.
39. Yu JK & Holland LZ (2009) Amphioxus whole-mount in situ hybridization. *Cold Spring Harb Protoc* 2009(9):pdb prot5286.

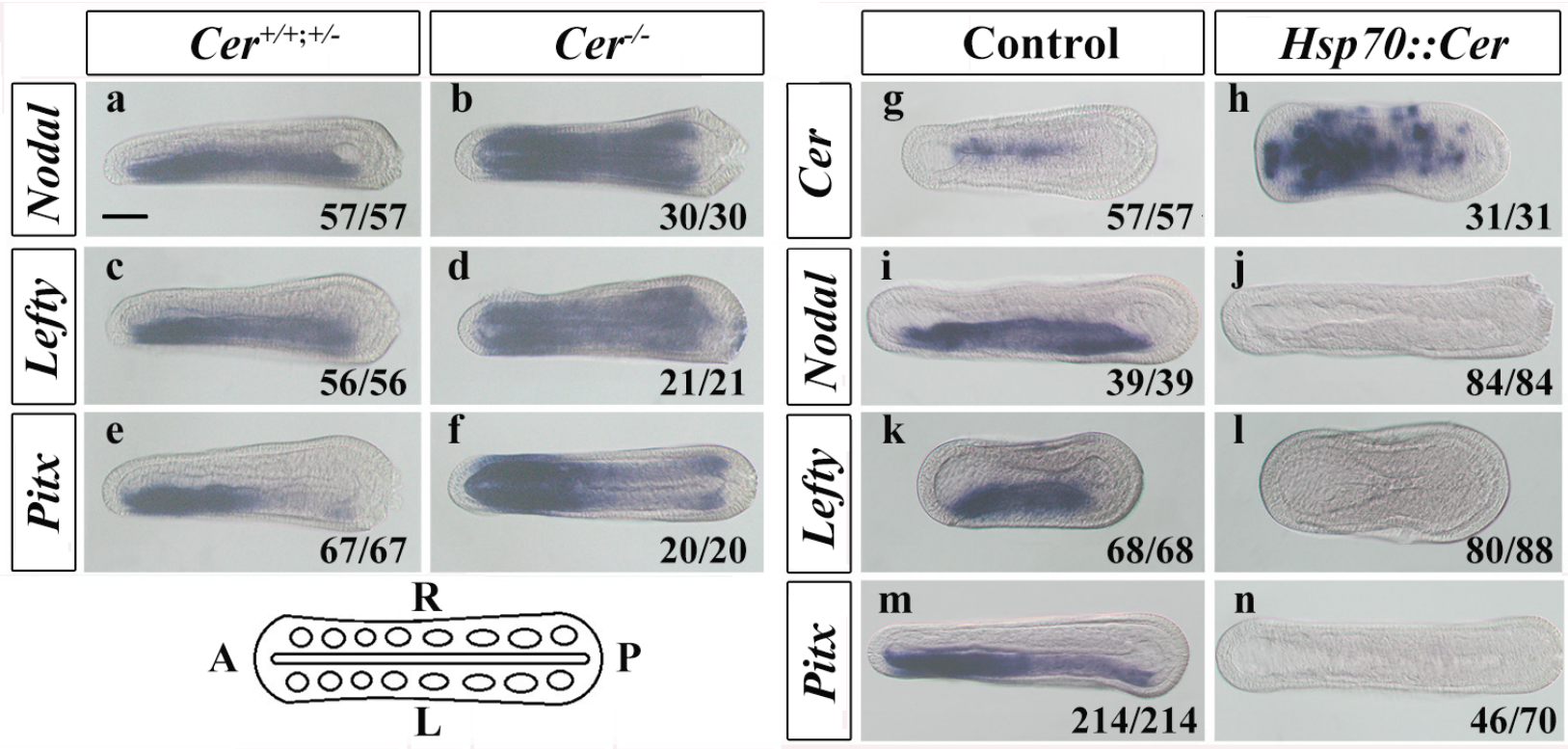
Cer+/+;+/-
Cer-/-
Control
Hsp70::Cer
Nodal
Lefty
Pitx
Cer
a
b
c
d
e
f
g
h
i
j
k
l
m
n
57/57
30/30
56/56
21/21
67/67
20/20
57/57
31/31
39/39
84/84
68/68
80/88
214/214
46/70
R
A
P
L

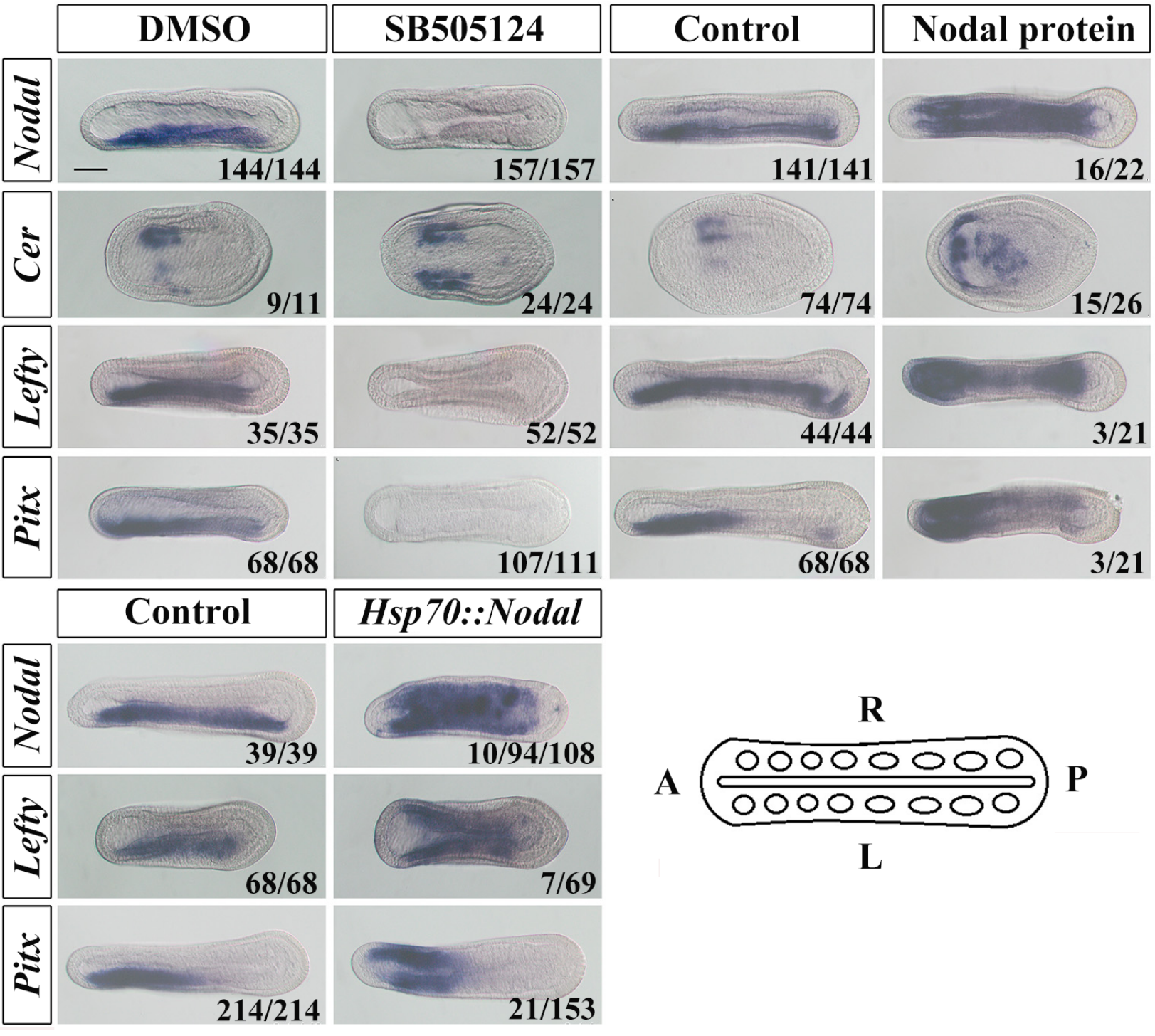
DMSO
SB505124
Control
Nodal protein
Nodal
Cer
Lefty
Pitx
144/144
157/157
141/141
16/22
9/11
24/24
74/74
15/26
35/35
52/52
44/44
3/21
68/68
107/111
68/68
3/21
Control
Hsp70::Nodal
Nodal
Lefty
Pitx
39/39
10/94/108
68/68
7/69
214/214
21/153
R
A
P
L

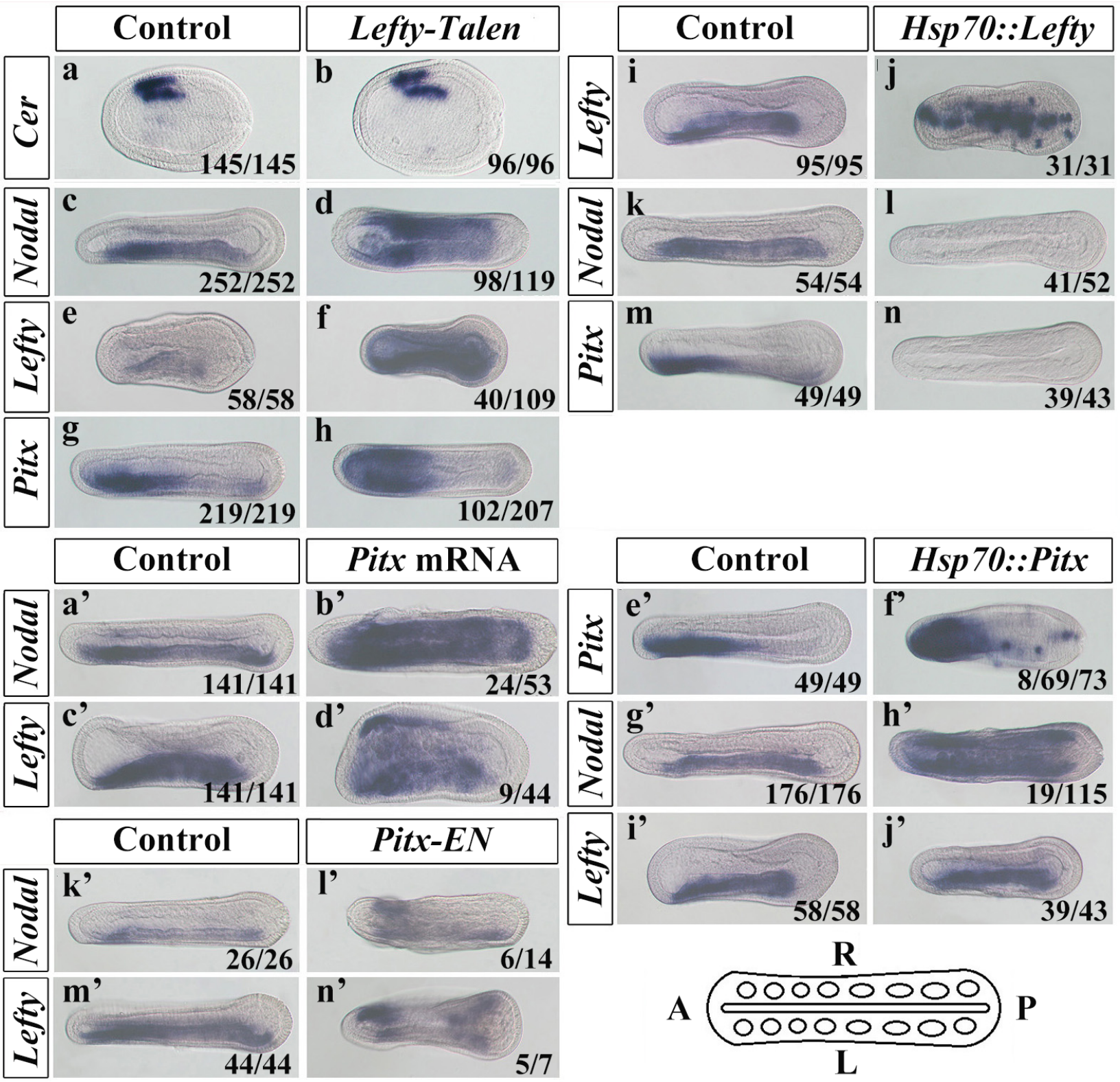
Control
Lefty-Talen
Control
Hsp70::Lefty
Cer
Nodal
Lefty
Pitx
a
145/145
b
96/96
c
252/252
d
98/119
e
58/58
f
40/109
g
219/219
h
102/207
Lefty
Nodal
Pitx
i
95/95
j
31/31
k
54/54
l
41/52
m
49/49
n
39/43
Control
Pitx mRNA
Control
Hsp70::Pitx
Nodal
Lefty
Pitx
Nodal
Lefty
a'
141/141
b'
24/53
c'
141/141
d'
9/44
e'
49/49
f'
8/69/73
g'
176/176
h'
19/115
i'
58/58
j'
39/43
Control
Pitx-EN
Nodal
Lefty
k'
26/26
l'
6/14
m'
44/44
n'
5/7
R
A
P
L

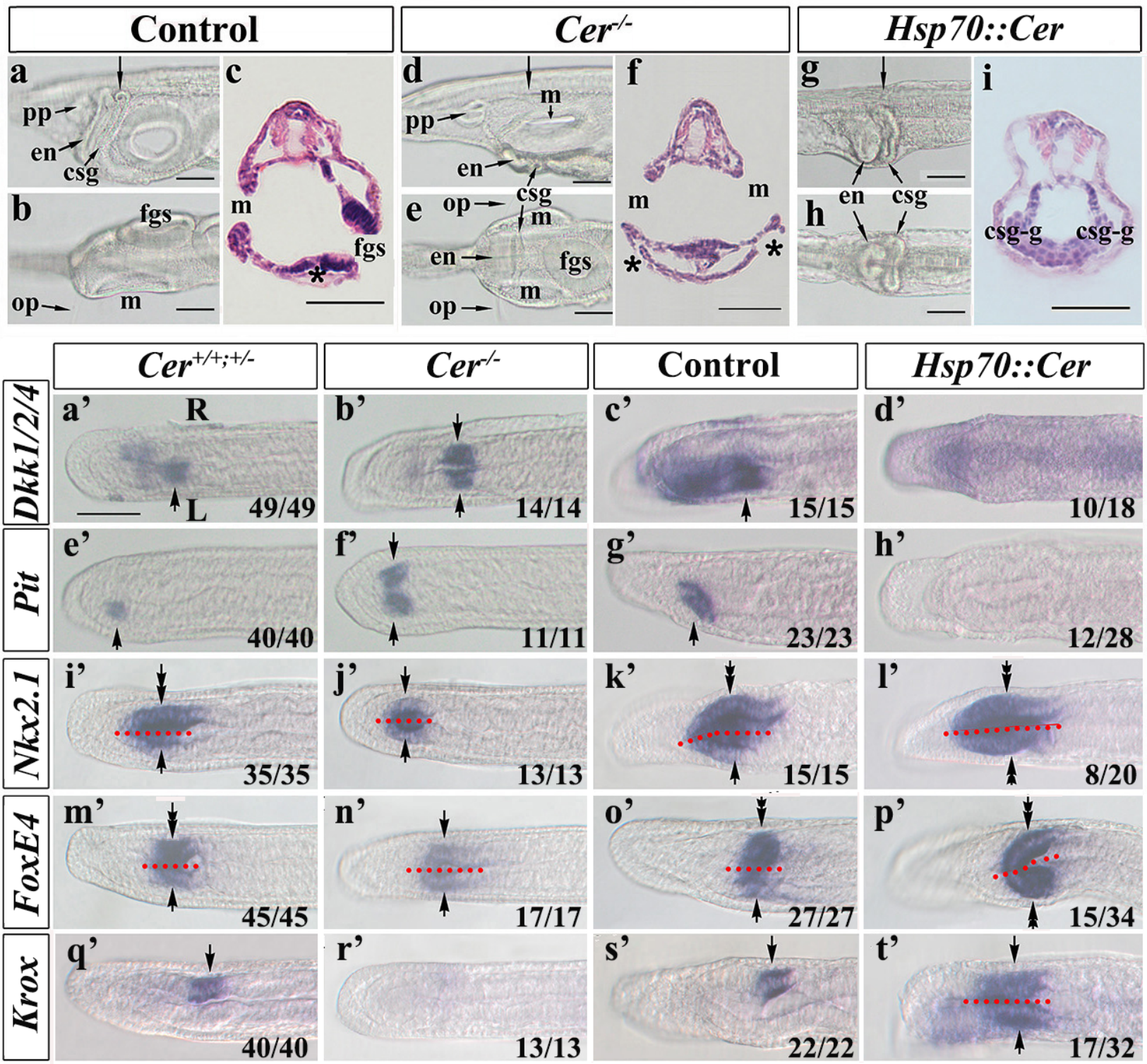
Control
Cer-/-
Hsp70::Cer
a
pp
en
csg
b
fgs
op
m
c
m
fgs
*
d
m
pp
en
csg
e
op
m
en
fgs
op
m
f
m
m
*
*
g
en
csg
h
i
csg-g
csg-g
Cer+/+;+/-
Cer-/-
Control
Hsp70::Cer
Dkk1/2/4
Pit
Nkx2.1
FoxE4
Krox
a'
R
L
49/49
b'
14/14
c'
15/15
d'
10/18
e'
40/40
f'
11/11
g'
23/23
h'
12/28
i'
35/35
j'
13/13
k'
15/15
l'
8/20
m'
45/45
n'
17/17
o'
27/27
p'
15/34
q'
40/40
r'
13/13
s'
22/22
t'
17/32

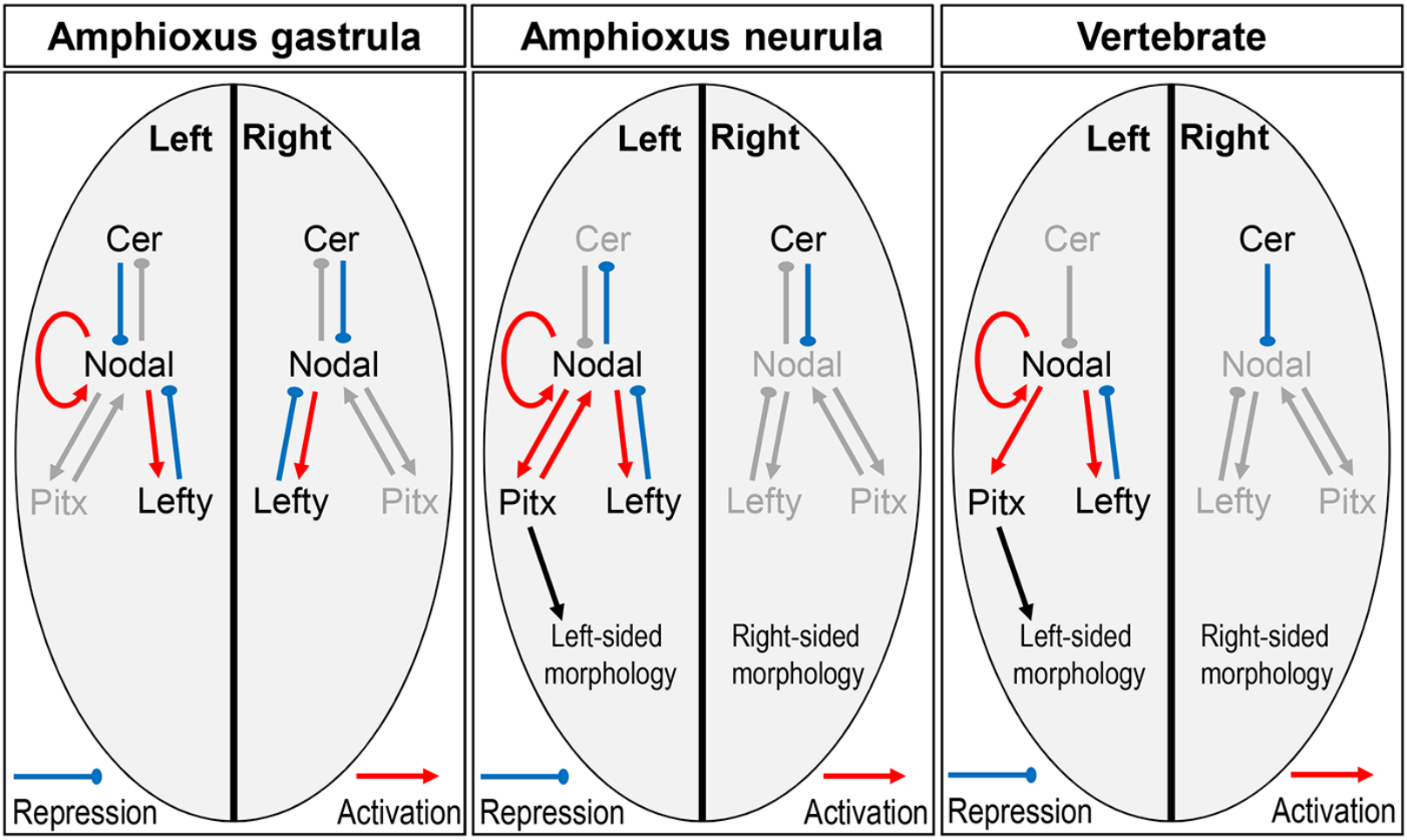
Amphioxus gastrula
Amphioxus neurula
Vertebrate
Left
Right
Cer
Nodal
Pitx
Lefty
Left-sided morphology
Right-sided morphology
Repression
Activation

Title: A *Cerberus-Nodal-Lefty-Pitx* signalling cascade controls Left-Right asymmetry in amphioxus

Short title: Left-Right asymmetry in amphioxus

Guang Li[1, §], Xian Liu[1, §], Chaofan Xing[1], Huayang Zhang[1], Sebastian M. Shimeld[2*], Yiquan Wang[1*]

[1] State Key Laboratory of Cellular Stress Biology, School of Life Sciences, Xiamen University, Xiangan District, Xiamen, Fujian 361102, China
[2] Department of Zoology, University of Oxford, The Tinbergen Building, South Parks Road, Oxford OX1 3PS, UK
§ These authors contributed equally to this work.
* Corresponding authors: wangyq@xmu.edu.cn, sebastian.shimeld@zoo.ox.ac.uk

Supplementary Information Appendix

Materials and Methods

Larval cultivation and detection of *Cer* mutations in founder and F1 amphioxus

Embryos injected with Talen mRNAs targeting *Cer* were reared at 24˚C in 5 litre plastic barrels filled with about 4 litres of filtered sea water and supplied with continuous air bubbling. After mouth opening, these larvae (we call them founders) were fed with unicellular algae *Dicrateria zhanjiangensis* (5-20 ml per time) twice a day. By 20 days after fertilization (around 8-gill slit stage), the animals were supplied with fine sand (2 cm thick) and fed with unicellular algae mixtures (*Platymonas sp*. and *Dicrateria zhanjiangensis*) twice a day. After metamorphosis (about 40 days after fertilization), the juveniles were reared as previous description (1, 2) till gonads became obvious. When the gonads developed to medium/large sizes, they were transferred to 20 ˚C plastic barrels for at least one week rearing before spawning induction (1). Gametes of each founder were collected individually and crossed with a wild-type animal respectively. After mid-neurula stage, 30-50 embryos of each cross were collected and analysed by PCR using Animal Tissue Direct PCR Kit (Foregene Co., China). Mutation efficiency and mutant sites of individuals were determined by restricted digestion and sequencing as previously described (1). The progeny (F1) carrying frame-shift mutations were maintained. When F1 grew up to around 3 centimetres in length, a tiny of individual tail tips were cut off for PCR amplification using above kit. After mutation diagnosis with restriction endonucleases, the mutation type of each individual was further determined by sequencing. Animals carrying identical frame-shift mutation were reared in a same tank, and inbreeding was carried out to generate F2 generation when F1 grew up to ripe adults, The F2 embryos were fixed at required developmental stages with 4% PFA-MOPS-EGTA for *in situ* hybridization analysis or morphological examination.

Plasmid construct preparation

To clone the full-length coding sequences of *Cer*, *Nodal*, *Lefty* and *Pitx* genes into relevant expression vectors, a set of primers embedded with different restriction enzyme sites were synthesized according to the sequence data retrieved from the NCBI database. The coding sequences of each gene were separately amplified from a gastrula cDNA library and then ligated into a pGEM-T-Easy vector (Promega Co.). After verification by sequencing, each of the coding sequences was cut off from the pGEM-T-Easy construct and ligated into an expression vector pXT7. Sequences were also re-amplified from the pGEM-T-Easy constructs, and cloned into a modified P1 construct restricted by *BamH*I and *Spe*I to generate *Hsp70::Cer*, *Hsp70::Nodal*, *Hsp70::Lefty* and *Hsp70::Pitx* constructs. The P1 construct was initially made from the vector pAcGFP1-1 (Clontech Co.) by integrating a 790 bp regulatory region of *B. belcheri Hsp70* gene upstream the GFP coding sequence in our previous study (3), and was modified by adding a *Spe*I site after GFP stop codon. To make a *Pitx* dominant negative construct, we first cloned the *Drosophila* Engrailed repressor domain (EnR) into the pXT7 vector, and then inserted sequence encoding Pitx DNA-binding domain ahead of the EnR encoding region. TALENs targeting *Cer* and *Lefty* genes were designed and assembled as previously described (3).

SB505124 and Nodal protein treatment

SB505124 (Sigma Co.) was dissolved at 20 mM in dimethyl sulfoxide (DMSO) and recombinant mouse Nodal protein (R&D Co.) was dissolved at 250 ngμL^{-1} in sterile 1 mM HCL containing 0.2% bovine serum albumin. Embryos were treated with 50 μM SB505124 or 8 μgml^{-1} Nodal protein (final concentration) in four-well dishes (coated with 1.5% agarose) from early gastrula to 8-somite stages, and then washed with filtered seawater three times. Before the treatment, fertilization envelope was removed by pipetteing embryos very gently with a yellow micropipette tip to facilitate the reagent accessing the embryo. Embryos were also treated with equal amounts of DMSO or 1 mM HCL and used as a negative control. The treated embryos were collected and fixed at either 3- or 8-somite stages for *in situ* hybridization analysis, or cultured continuously for morphological phenotype observation.

***In situ* hybridization**

Embryos at desired developmental stages were fixed in 4% PFA-MOPS-EGTA and then stored in 80% ethanol in PBS at -20°C until needed. The pGEM-T-derived plasmids containing amphioxus *Cer*, *Nodal*, *Lefty* or *Pitx* coding regions were linearized by restriction enzyme digestion and applied to synthesize a digoxigenin (DIG)-labeled (Roche Co.) antisense riboprobe with Sp6 or T7 RNA polymerase (Promega, USA). Whole-mount *in situ* hybridization (WISH) was performed essentially as previously described (5). After staining, the embryos were washed with PBS, mounted in 80% glycerol and photographed using an inverted microscope (Olympus Co.).

References

1. Li G, Shu Z, & Wang Y (2013) Year-round reproduction and induced spawning of Chinese amphioxus, Branchiostoma belcheri, in laboratory. *PLoS One* 8(9):e75461.
2. Li G, Yang X, Shu Z, Chen X, & Wang YQ (2012) Consecutive spawnings of Chinese amphioxus, Branchiostoma belcheri, in captivity. *PLoS One* 7(12):e50838.
3. Li D, *et al.* (2012) Isolation and functional analysis of the promoter of the amphioxus Hsp70a gene. *Gene* 510(1):39-46.
4. Li G, *et al.* (2014) Mutagenesis at specific genomic loci of amphioxus Branchiostoma belcheri using TALEN method. *J Genet Genomics* 41(4):215-219.
5. Yu JK & Holland LZ (2009) Amphioxus whole-mount in situ hybridization. *Cold Spring Harb Protoc* 2009(9):pdb prot5286.

Supplementary Tables

Table S1. Primers used for making pGEM-T Easy and pXT7 constructs

Genes	Primer sequences (5'→3')	Enzyme site added
Cer	Forward: GGTACCATGAAGACGAGCGTGAGGAGC	*Kpn*I
	Reverse: ACTAGTTCAGAAGTACTTATCCCCACATG	*Spe*I
Nodal	Forward: GGTACCGCAGGCCGAGACCAACACCGC	*Kpn*I
	Reverse: ACTAGTCTACTGACAGCCGCATTCATCC	*Spe*I
Lefty	Forward: CTCGAGTACGATGAAACCTGTTCTAGTT	*Xho*I
	Reverse: ACTAGTTTACTGTGTGCACGCACACTG	*Spe*I
Pitx	Forward: GGTACCACATATCTAAGGAGGACATCGTG	*Kpn*I
	Reverse: ACTAGTTCTTTAGCAAACAAATCCCATACGC	*Spe*I

Table S2. Primers used for making Hsp70 constructs

Genes	Primer sequences (5'→3')	Enzyme site added
Lefty	Forward: GGATCCTACGATGAAACCTGTTCTAGTT	*Bam*HI
	Reverse: GCGGCCGCACTAGTTTACTGTGTGCACGCACACTG	*Not*I-*Spe*I
Cer	Forward: GGTACCATGAAGACGAGCGTGAGGAGC	*Kpn*I
	Reverse: ACTAGTTCAGAAGTACTTATCCCCACATG	*Spe*I
Nodal	Forward: GGATCCGCAGGCCGAGACCAACACCGC	*Bam*HI
	Reverse: GCGGCCGCCTACTGACAGCCGCATTCATCC	*Not*I
Pitx	Forward: GGTACCACATATCTAAGGAGGACATCGTG	*Kpn*I
	Reverse: ACTAGTTCTTTAGCAAACAAATCCCATACGC	*Spe*I

Table S3. Primers used for making *Pitx-EN* construct

Genes	Primer sequences (5'→3')	Enzyme site added
Pitx	Forward: GGTACCACATATCTAAGGAGGACATCGTG	*Kpn*I
	Reverse: GAATTCTCCCAGCTGATTTCGCTCGCG	*EcoR*I

Table S4. Primers used for amplifying gene fragments including TALEN target sites

Genes	Primer sequences (5'→3')	Amplicon sizes (bp)
Cer	Forward: ATGAAGACGAGCGTGAGGAGC	427
	Reverse: CATCATCACCTGGAAGACGG	
Lefty	Forward: GAAACCTTCGCAGCAACATCG	376
	Reverse: CGACACGGGTAATTTGGAGC	

Table S5. *Cer* and *Lefty* TALEN binding sequences

Target gene	Target site sequence	Restriction enzyme used
Cer	TTTCAGACTCTCGGGTTGATT*CGGCCG*CCAGTCGGGAGGGGTCGGGACGGA	*Eag*I
Lefty	TTCTCGTGTGTTCTGGCCAGCG*CCTTGG*CGTTCTCGGCGGACCACGTCA	*Sty*I

Supplementary Figures

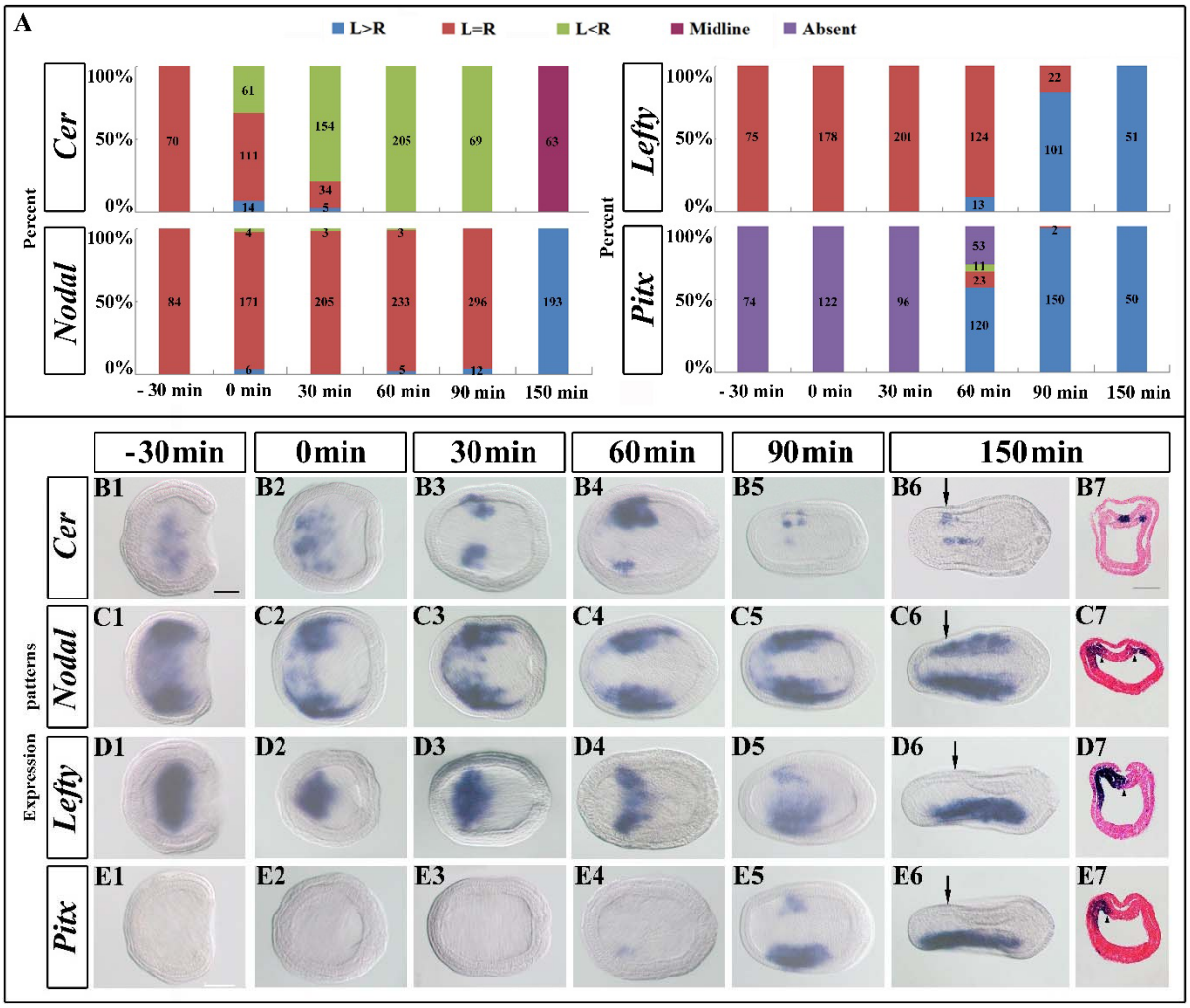

Fig. S1. Sequential onset of asymmetric expression of *Cer*, *Nodal*, *Lefty* and *Pitx* in amphioxus embryos. (A) Percentages of embryos showing each type of expression patterns (L>R, L = R, L < R and absent) for *Cer*, *Nodal*, *Lefty* and *Pitx* at 6 developing stages. Time at the late gastrula stage is defined as the 0 minute, and one stage before and 4 stages after that were adopted in the analysis. Following *in situ* hybridization, embryos were classified into right bias (R > L), equal distribution (R = L), left bias (R < L), or none (absent) of signals across the LR axis. Bars represent percentages; numbers of embryos analyzed are indicated on each bar. (B1-B6) Representative examples of *Cer* expression patterns at six developing stages. Arrow in (B6) marks the section plane in (B7). (B7) Transverse section of an embryo, showing *Cer* expression in the floor plate and several cells of the right first pre-somite. (C1-C6) Representative examples of *Nodal* expression patterns at six developing stages, note symmetric expression through early stages, with higher left-sided expression only visible in the oldest embryos. Arrow in (C6) marks the section plane in (C7). (C7) Transverse section of en embryo, showing *Nodal* expression in the left and right pre-somites. (D1-D6) Representative examples of *Lefty* expression patterns at six developing stages. Arrow in (D6) marks the section plane in (D7). (D7) Transverse section of an embryo, showing *Lefty* expression in the left first pre-somite and the regions adjacent to it, including the left side of dorsal-lateral endoderm, axial mesoderm and ectoderm. (E1-E6) Representative examples of *Pitx* expression patterns at six dveloping stages. Arrow in (E6) marks the section plane in (E7). (E7) Transverse section of an embryo, showing *Pitx* expression in the left pre-somites. Images in panels B, C, D and E are taken from the dorsal view with anterior to left. Scale bar (50 μm) in B1 applies to all panels.

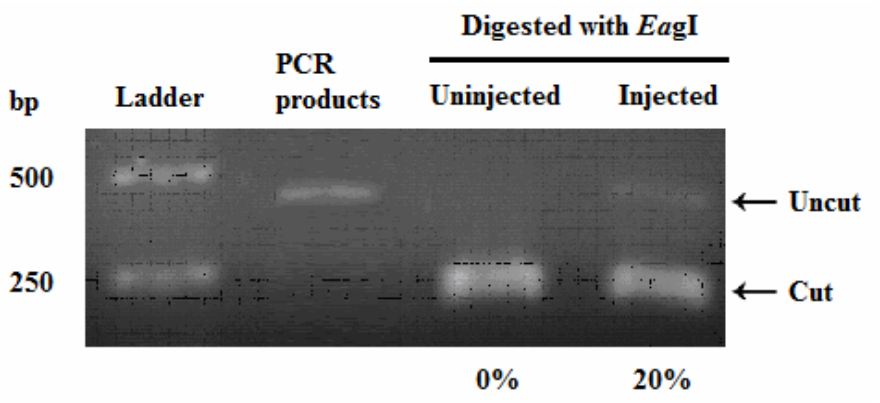

Fig. S2. Mutation rates of *Cer* TALEN in F0 embryos. Aout 30 embryos at mid-neurula stage were randomly collected for DNA extraction and PCR amplification. PCR products were digested with *Eag*I (which cuts within the TALEN engineered segment of DNA: see *SI Appendix*, Fig. S3). The uncut:cut ratio was estimated roughly as an indication of the mutation efficiency and labeled below the gel image. As expected, PCR products from the uninjected embryos were completely cut by *Eag*I, but approximately 20% of PCR products from the TALEN mRNA injected embryos were uncut.

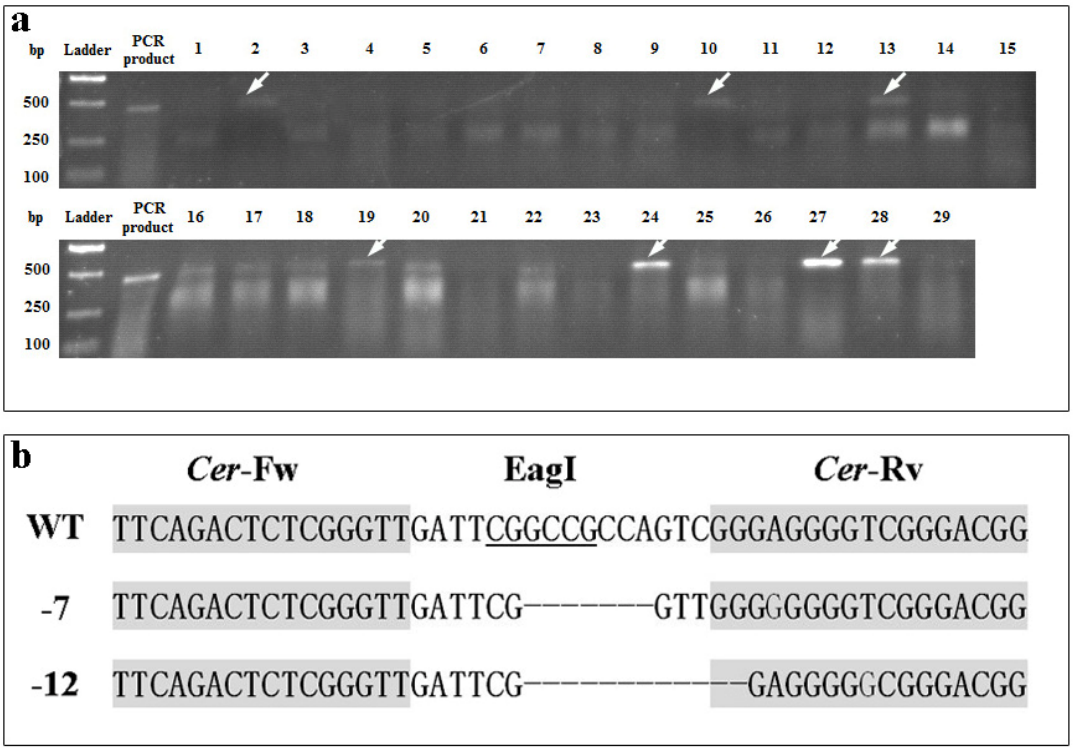

Fig. S3. *Cer* TALEN F1 animal screening (a) and genotype determination (b). Genotypes of twenty-nine animals were first analyzed using PCR product cleavage assay, and the animals carrying mutations at the target locus (marked by arrows) were further determined by DNA sequencing. Among the seven animals carrying mutations, three are $Cer^{-7/0}$ heterozygotes (showing a deletion of 7 bp in panel b) and one is a $Cer^{-12/0}$ heterozygote. The three $Cer^{-7/0}$ heterozygotes were used for further analysis in this study.

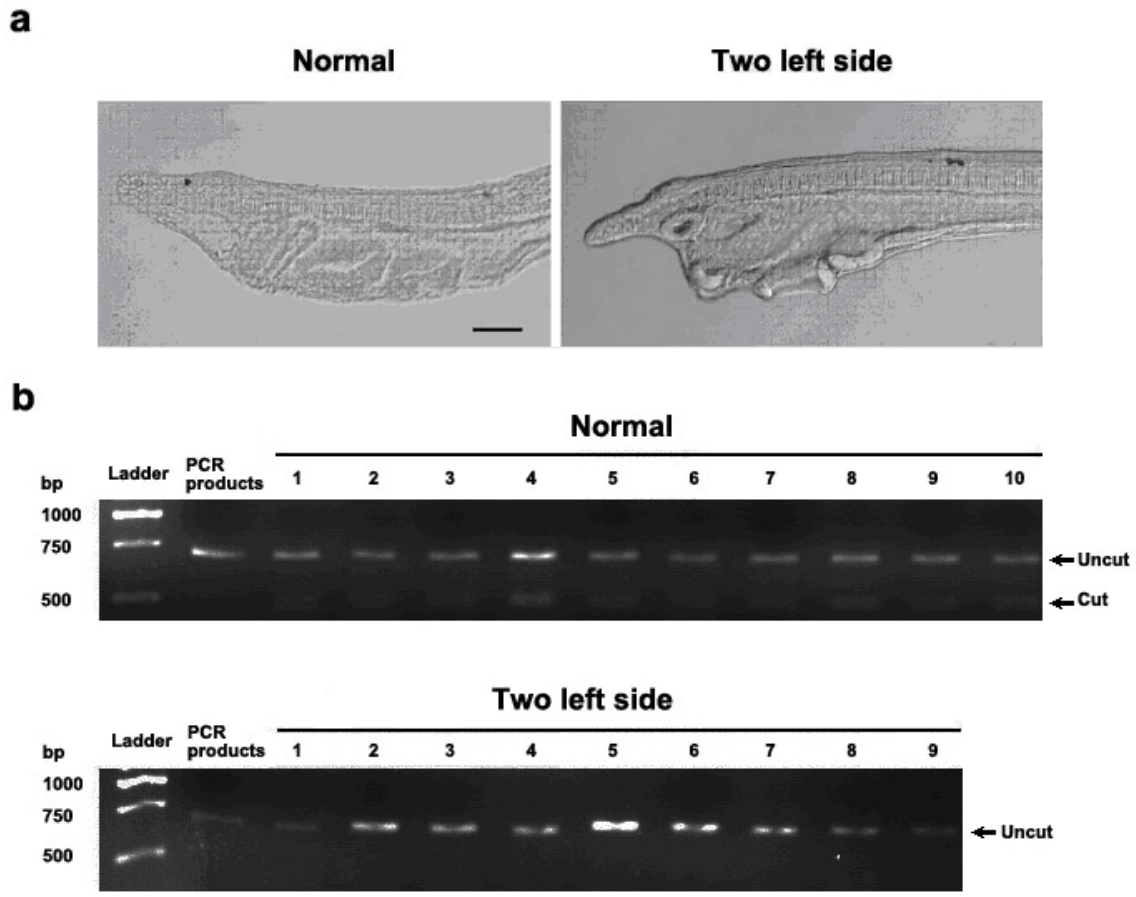

Fig. S4. Phenotype (a) and genotype (b) of TALEN *Cer* F2 animals. (a) Phenotype analysis revealed that the offspring from *Cer*$^{-7/0}$ inbreeding were born according to the correct Mendelian ratio: among the 584 animals analyzed, 134 showed two left side phenotype (see also *SI Appendix*, Fig. S7 and Fig. S5), while all others showed a wild type phenotype with mouth formed on the left side and endostyle on the right. This dose not significantly differ from the expected Mendelian ration of 3:1 ($p>0.25$; Chi-squared test). (b) Genotype analysis of 19 larvae revealed that larvae with normal LR asymmetry are *Cer*$^{-7/0}$ heterozygous (10/10), while larvae with the two left side phenotype are *Cer*$^{-7/-7}$ homozygotes (9/9). PCR products amplified from each of these 19 larvae were first digested with *Eag*I enzyme and then analyzed by gel electrophoresis. As shown in the image, about half of the PCR products deriving from larvae with normal phenotype (lanes 1-10) were digested by *Eag*I, but all of the product from larvae with the two left side phenotype were uncut.

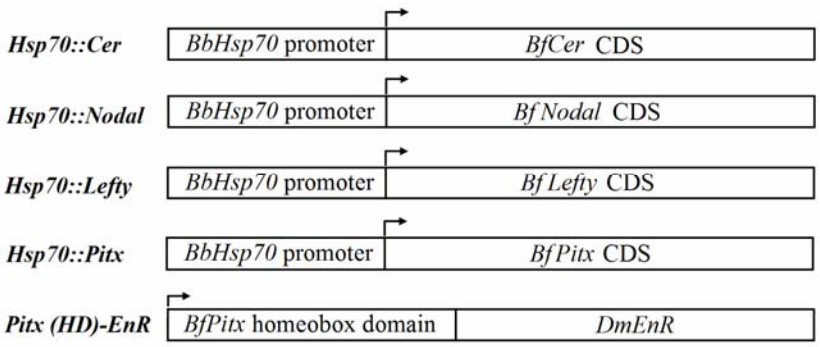

Fig. S5. Schematic representation of *Hsp70::Cer/Nodal/Lefty/Pitx* and *Pitx (HD)-EnR* constructs. Arrows indicate the transcription start sites. For *Hsp70::Cer/Nodal/Lefty/Pitx* constructs, transcription is driven by *B. belcheri Hsp70* gene promoter, and for *Pitx (HD)-EnR* construct, transcription is driven by a T7 promoter for in vitro RNA synthesis.

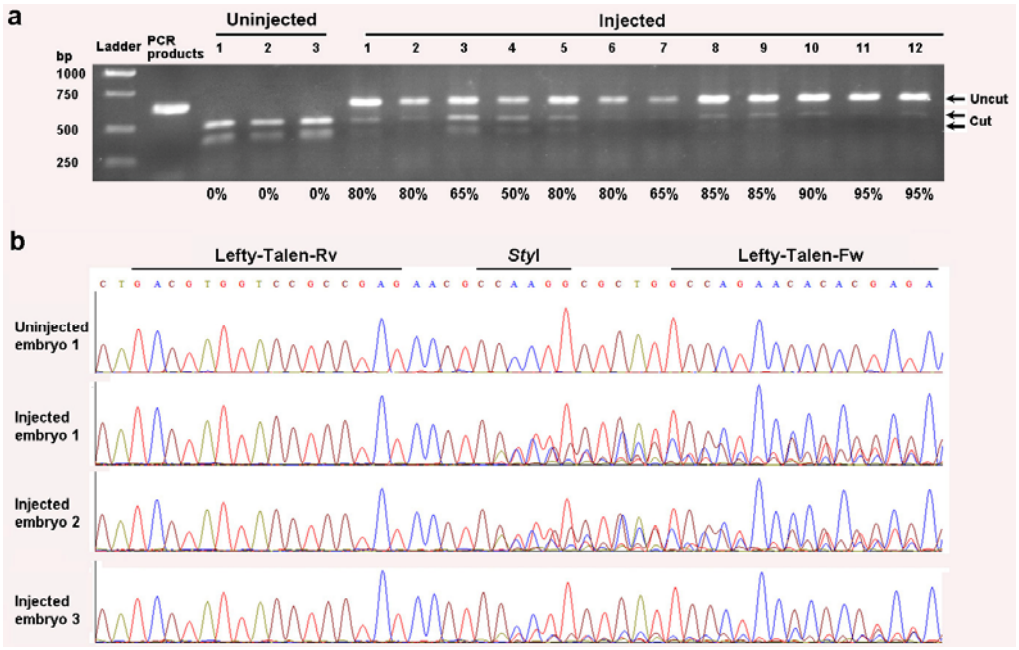

Fig. S6. Mutation ratios (a) and target sequences (b) of *Lefty* TALEN mRNA injected embryos. The mutation ratios of each embryo are assessed with PCR-restricted digestion since injection of TALEN mRNA into a zygote usually generates a mosaic individual. After injection with *Lefty* TALEN mRNAs, three un-injected and twelve injected embryos with normal morphology were randomly selected at mid-neurula stage and lysed separately using Animal Tissue Direct PCR Kit (Foregene Co., China). Fragments spanning the target site were amplified and then digested with restriction enzyme *Sty*I. The mutation efficiencies of each embryo were estimated by uncut:cut ratios shown under the gel image. As shown in image (a), PCR products from the three un-injected embryos were completely digested and more than 50% of PCR products from injected embryos were uncut. To verify the targeting specificity, the PCR products from the uninjected embryo 1 and three injected embryos were directly sequenced. As shown in image (b), the uninjected embryo 1 displays a uniform single peak throughout the sequence, and three injected embryos show multiple peaks after mutation site, indicating a site specific mutation.

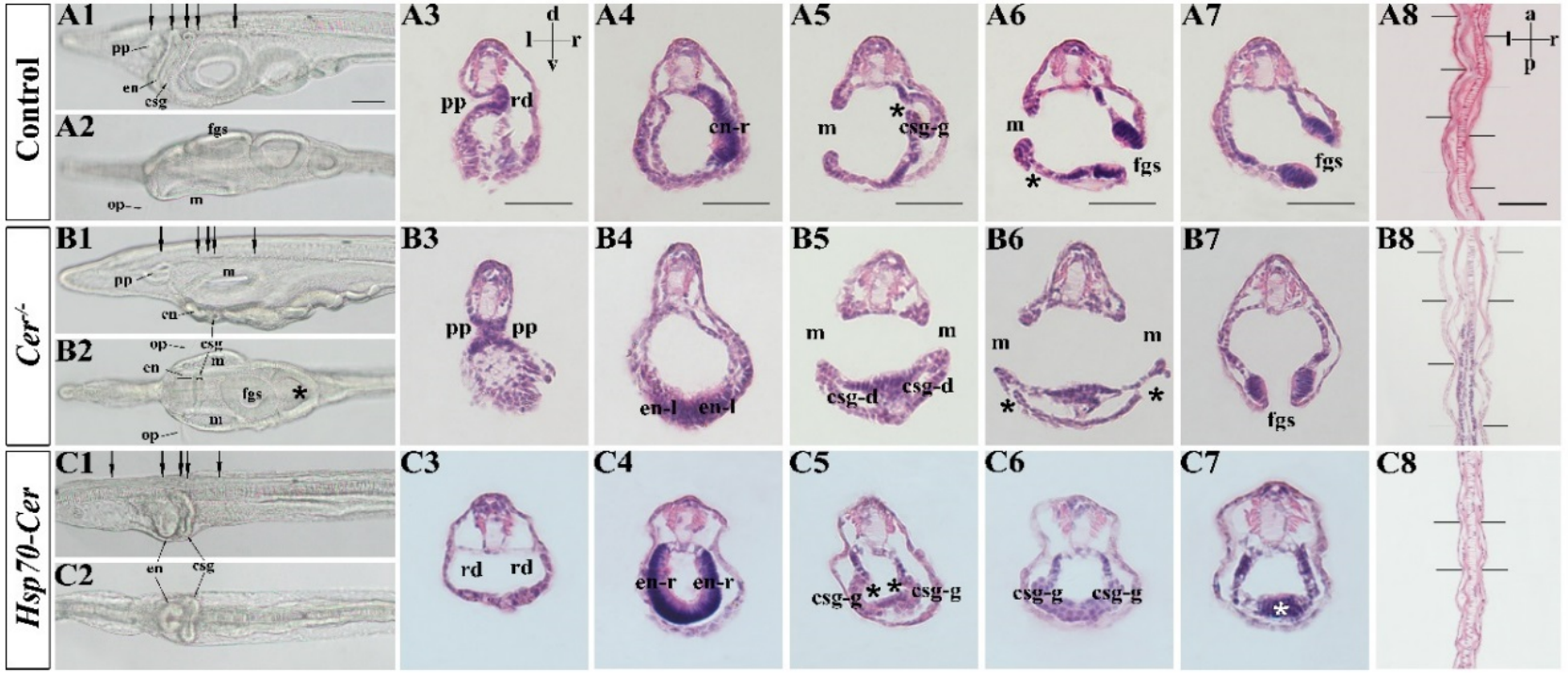

Fig. S7. *Cer* mutation or misexpression causes LR defects in amphioxus larvae. Panels A1, A2, A6, B1, B2, B6, C1, C2 and C6 are replicated from Fig. 4 for comparison. (A1-A8) Asymmetrical morphologies of control larvae (as seen in wild-type, *Cer*$^{+/-}$ or *Hsp70*::*Cer*-injected but not heat-hocked larvae). (A1) Left lateral view of pharyngeal region focused on the right side, showing the left-sided pre-oral pit (pp), right-sided endostyle (en) and club-shaped gland (csg). Arrows mark the section planes in (A3-A7). (A2) Dorsal view of pharyngeal region focused on the ventral side, showing the left-sided mouth(m) and oral papillar (op) and right-sided first gill slit (fgs). (A3) shows the left-sided pre-oral pit (pp) and right-sided right diverticulum (rd); (A4) shows the right part of endostyle (en-r); (A5) shows the left-sided mouth (m) right-sided glandular region of CSG (csg-g) and its internal opening (asterisk); (A6) shows the left-sided mouth (m), the external opening of CSG (asterisk) and the right-sided the first gill slit (fgs). (A7) shows the right-sided first gill slit (fgs). (A8) Longitudinal section of a 3-gill-slit-stage larva, showing the asymmetrical arrangement of the somites along A-P axis. (B1) Left lateral view of pharyngeal region focused on the sagittal plane, showing the left-side pre-oral pit (pp), mouth (m) and improperly developed endostyle (en) and CSG. Arrows mark the section planes in (B3-B7). (B2) Dorsal view of pharyngeal region focused on the ventral side, showing the duplicated mouths (m), oral papillae (op), left-side parts of the endostyle (en), CSG, and ventrally located the first (fgs) and second (asterisk) gill slits. (B3) shows the duplicated pre-oral pits (pp); (B4) shows the morphological symmetry of endostyle, resulting from the duplication of left-side endostyle (en-l); (B5) and (B6) show the duplicated mouths and ducts of

the CSG (csg-d). Two external openings of CSG (asterisks in B6) appear on both sides; (B7) shows the first gill slit (fgs) ventrally located. (B8) Longitudinal section of 3-gill-slit-stage *Cer* mutant larva, showing the symmetrical arrangement of somite along theA-P axis. (C1) Left lateral view of pharyngeal region focused on the sagittal plane, showing the improperly developed endostyle (en) and CSG (csg). No mouth opening and pre-oral pit are observed. Arrows mark the section planes in (C3-C7). (C2) Dorsal view of pharyngeal region focused on the ventral side, showing the morphological symmetry of endostyle and CSG, resulting from duplication of the right-side parts of endostyle and CSG. (C3) shows the duplicated right diverticulum (rd); (C4) shows the morphological symmetry of endostyle, resulting from the duplication of right-side part endostyle (en-r); (C5) and (C6) show the symmetrical feature of CSG, resulting from the duplication of right-sided glandular region (csg-g). Two internal openings of the CSG (asterisks in C5) appear on both sides; (C7) shows the first gill slit ventrally located. (C8) Longitudinal section of 3-gill-slit-stage *Cer* misexpressed larva, showing the symmetrical arrangement of somite along theA-P axis. All scale bars are 50 μm and are applicable to the panels in same column. Direction indicated in panel A3 (d, dorsal; v, ventral; l, left; and r, right) applies to all panels in the five middle columns, and that in panel A8 (a, anterior, p, posterior, l, left; and r, right) applies to panels B8 and C8. Black horizontal lines in A8, B8 and C8 mark the boundary between somitic segments